

Thin Floor Milling Using Moving Support

Jixiong Fei (✉ tjujackfei@163.com)

CAEP

Bin Lin

Tianjin University

Tian Huang

Tianjin University

Juliang Xiao

Tianjin University

Research Article

Keywords: High speed milling, thin floor, moving support, robot assisted machining

Posted Date: September 21st, 2021

DOI: <https://doi.org/10.21203/rs.3.rs-893942/v1>

License:   This work is licensed under a Creative Commons Attribution 4.0 International License.

[Read Full License](#)

Version of Record: A version of this preprint was published at The International Journal of Advanced Manufacturing Technology on February 2nd, 2022. See the published version at <https://doi.org/10.1007/s00170-022-08814-z>.

Abstract

During milling the thin floor of a pocket which locates on a monolithic structure, it is very difficult to achieve high accuracy and good surface quality due to its low rigidity. In this paper, a novel approach is proposed to overcome the difficulties that encountered during milling of the thin floor. The method is realized by using small axial depth of cut but placing a moving support at the back surface of the thin floor during machining, in which the support will move with the cutter at the same velocity. An experimental platform is built to demonstrate the validation of the proposed method. The experimental results show that the proposed method can effectively improve the accuracy and surface quality during milling the thin floor of a pocket of the monolithic structure.

1. Introduction

Flexible monolithic thin-walled workpieces with multi-pockets are widely used in the engineering practice, especially in the aerospace engineering. The multi-pocket structure is used to reduce the weight of the component yet to its stiffness and strength. Typical application of the multi-pocket structure includes the rocket tanks and the airplane fuselage as shown in Fig. 1. The remaining wall thickness of the pocket, which refers to the normal distance from the outer and inner surface of the pocket after machining, is important to compromise the weight reduction and the strength. It becomes an important dimension requirement during machining. However, the cutting vibration and deformation, which are mainly caused by the low rigidity of thin floor, will make it difficult to achieve desirable surface quality and accuracy after machining [1].

Usually, a flexible monolithic component with pockets is manufactured by two different methods. For the first one, the pockets are firstly obtained by the high speed milling process on a flat blank block. At this stage, the block is usually fixed flatly on the worktable of a machining center. Thereafter, the blank with pockets is formed to the desirable shape by bending or other metal forming process. The whole process is shown in Fig. 2.

For this method, the thin floor of a pocket is supported by the worktable surface and its stiffness along the axial direction of the milling cutter is therefore strengthened during machining. The undesirable vibration of the thin floor along the axial direction is thus suppressed. However, the axial depth of cut can't be too large during milling the thin floor. If the axial depth of cut is too large, the remaining thickness of the floor will become thinner and thinner (as shown in Fig. 3) and even be cut through due to the increasing axial depth of cut [3]. Besides, forming flaws will easily occur due to uneven distribution of block workpiece materials because of the pocket structures, especially at the intersection part of several ribs as shown Fig. 4. This makes the component fail to meet the strict standard of the aerospace components.

Different from the first method, the second one firstly forms the blank block to the desirable shape, and then machines the pocket structures to reach the final accuracy. The whole process is shown in Fig. 5.

The problem encountered in this method is to fix the workpiece. The fixture has two intentions for this method, namely, to fix the workpiece as well as to reinforce the low stiffness of the thin floor and thus to reduce the undesirable vibration during machining. However, after the blank is formed to the desirable shape, it becomes very difficult to clamp because of its complex surface. Besides, the inappropriate fixture condition may lead to the undesirable deformation of the block before machining and thus the deformation will be released after machining, which will lead to poor dimensional or shape error.

To clamp the workpiece properly, many methods were presented in academic and engineering. One possible one was the so called mold design method [4]. This method aimed to design a giant mold whose inside surface has the same shape with the back surface of the workpiece (as shown in Fig. 6 (a)) to support the flexible workpiece. Obviously, large axial depth of cut can't be used since the floor may be cut through as shown in Fig. 3. Besides, it lacks flexibility since for a different workpiece, the mold support needs to be redesigned and reproduced. Sometimes, coatings, foams or wax were used to replace the mold to strengthen the workpiece [5]. Recently, Kolluru and Axinte [6, 7] proposed that use a novel ancillary device to reinforce the whole surface of the workpiece as shown in Fig. 7. The method consisted of distributed mass blocks, viscous tape and torsion springs. The springs tensioned and placed in casing exert a radial force, acting as inertia force on casing. A conformable damping sheet such as neoprene were pressed against the casing using the torsion springs provides stiffness during vibration of casing due to stretching of neoprene sheet between the springs. Moreover, the viscoelastic nature of the neoprene sheet provides damping to the casing. Henceforth, mass, stiffness and damping are imparted to the thin wall structure without having the residual viscoelastic tape problem.

Except for the mold design method, multi-support method was developed as shown in Fig. 6 (b) [8], several fixture elements or dampers were attached to the key locations, such as the locations that have the largest mode displacement of the workpiece. This method can locally reinforce the stiffness of the workpiece. Compare to the mold design method, it is much more flexible. The fixture element of the multi-support method can be made as a matrix and thus it is suitable for support and clamp of the workpiece with complex surfaces. The investigation related to this method includes the fixture element number optimization, the layout of the fixture element, the applied force between the workpiece and the fixture element, the sequence of the fixture operation etc. Generally, it was treated as an optimization problem. Such as, Qin et al. [9] analyzed and optimized the clamping sequence of the fixture element. Their investigation considered the varying contact force and friction force during clamping. Chaari et al. [10] optimized the clamping force of the fixture based on the particle swarm optimization (PSO) method. Chen et al. [11] optimized the layout and the applied clamping force. A multi-objective model to reduce the maximum deformation and to increase the distributing uniformity of the deformation was established and was solved by the genetic algorithm (GA). Sundararaman et al. [12] optimized the layout of the fixture element combined the surface response method, which modeled the relationship between the maximum workpiece deformation and the locator position, and evolutionary techniques including GA and PSO methods. Yang et al. [13] also optimized the locating layout of the fixture element. The method is based on cuckoo search algorithm. Liu et al. [14] also optimized the number and the fixture layout element in the end milling process of the flexible workpiece. The optimization procedure consisted of

two stages. The first stage was to place the fixture element at the position with local maximum deformation. Thereafter, the number of the elements was reduced by a specified optimization method. Zeng et al. [15] also introduced a fixture design method, it can optimize the element location, the clamping force and the element number simultaneously.

For this method, the multi-support methods can locally increase the stiffness of the workpiece at some key locations. However, the axial depth of cut can't be too large or too small when the cutter locates at the area between two supports. If the axial depth of cut is too large, the remaining thickness of the thinner and thinner and even been cut through. On the other hand, if the axial depth of cut is too small, vibro-impact will occur between the floor and the cutting tool due to the separation in between and thus lead to poor surface quality [16, 17]. Moreover, it will take much time to clamp the workpiece. Besides, it is a difficult task to control so many fixture elements simultaneously.

The mold design method aims to support the whole back surface of the workpiece while the multi-support method aims to support the workpiece back surface at some key points with fixed elements. Different from these two methods, a novel method, which employs only one moving element to support the back surface of workpiece, is proposed in this investigation. The remaining part of the paper will focus on the schematic and the realization of the proposed method.

2. Proposed Method And Its Model

The schematic diagram of the proposed method is shown in Fig. 8. The axial depth of cut a_p is set to be much smaller than the remaining thickness of the thin floor. The aim is to avoid cut through of the thin floor. To avoid separation between the floor and the cutting tool, a fixture element is placed at the back surface of the thin floor. The axis of the support element will collinear with the axis of cutter. During milling process, the support element will move with the cutting tool at the same velocity, and the two axes will keep aligning with each other. Present method is similar to the double-sided milling method which was proposed by Shamoto et al [18, 19], in which the both sides of a thin plate are machined by a right and a left face milling cutter placed simultaneously. Recently, Fei et al. [20, 21] proposed that using the moving fixture to suppress the chatter vibration and workpiece deformation while Ozturk et al. [22] proposed that using the moving robot support to increase the production during machining. However, the method proposed in their investigation was used in thin wall machining.

During machining the thin floor, it will vibrate easily because of its low stiffness. If the vibration displacement of the cutter tip is larger than the small axial depth of cut, the cutter will separate from the floor, when the floor vibrate back, it will collide with the cutter and then the vibro-impact occurs, which will make serious damage to the machined surface quality as shown in Fig. 20(a). After a moving fixture element is used to support at the back surface of the workpiece, the vibration of the floor will be effectively prevented, and thus the contact lose between the floor and the cutter. The vibro-impact phenomenon can therefore be suppressed. Besides, the moving support will reinforce the local stiffness

of the workpiece and thus improve the system stability, which will result in better surface quality. The moving fixture will also decrease the floor deformation effectively, and thus decrease the form error.

Differences between present method and the existed multi-support methods are: (i) the fixture element is moving for present method while it is fixed for the existed methods; (ii) only one fixture needed while more than one element are needed for the existed methods. The advantages for the present method include: (i) the cost will be lesser than the multi-support method because lesser support elements are needed; (ii) the vibration and deformation will be decreased effectively because of the simultaneously moving of the fixture element with milling tools, unlike the multi-support system that the chatter and deformation still exists in the zone between two adjacent support elements. Besides, present method will cost less clamping time when compared to the multi-support method. However, it is not easy to let the cutter axis align perfectly with the fixture element axis, which may lead to a distance between the two axes and thus leads to the twist of the thin wall as shown in Fig. 9. To solve this problem, present paper has designed a support head which will be presented in the next section to remove this twist effect. The contact force between the support head and the floor is also very important. The contact force between the support head and the thin floor can't be too large or too small. If it is too large, there will be scratch on the back surface of the thin floor. Conversely, if it is too small, the cutter and the floor will still be separated. Following section will focus on the experimental setup based on the proposed schematic.

3. Experimental Validation

3.1 Experimental setup

An experimental setup is built to realize the method mentioned above. The setup is consisted of two five degree-of-freedom (DOFs) parallel robots where one of them is equipped with milling head while the other one is equipped with support head, the fixture module and the control module. The CAD model of the setup is shown in Fig. 10.

The milling robot used in the setup is called TriMule developed by Huang et al [23, 24]. Its configuration is similar to the Tricept and Exechon robot. The real milling robot and its corresponding mechanism schematic diagram are shown in Fig. 11. From the figure, it can be seen that the TriMule robot is consisted of a 1T2R spatial parallel mechanism plus an A/C type wrist.

The spatial parallel mechanism can be treated as a 6-DOF $\underline{U}PS$ limb plus a 2-DOF planar parallel mechanism which is composed of two actuated $\underline{R}PS$ limbs and a passive RP limb in between with its one end being rigidly fixed to the platform. The base link of the planar parallel mechanism is connected by a pair of R joints with the machine frame. Here, R, P, U, and S denote revolute, prismatic, universal, and spherical joints, and the underlined \underline{P} means an actuated prismatic joint respectively. The characteristics of the robot machining center include lower weight, higher speed, more flexibility etc.

The dimension of the robot machining center is shown in Table 1. The workspace of the milling robot is shown in Fig. 12. The tool interface of the spindle is HSK-E40 and a highest spindle speed of 24000 rpm,

a power of 7.5 KW and a torque of 7.2 Nm.

Table 1 Dimensional parameters of the robot (in meters).

a	b_x	b_y	e	l_1	l_2	d	H	h_1	h_2	R
0.135	0.320	0.570	0.345	0.120	0.220	0.190	1.000	0.240	0.220	0.620

The support robot is obtained by replacing the milling head of the machining robot with a support head. The real device and the corresponding schematic diagram of the support head shown in Fig. 13. The key parts of the support head [26] is the seven balls as shown in the figure. One of the seven balls locates at the central of the sleeve. The central ball is integrated with an ultrasonic thickness measurement sensor to measure the remaining thickness of the thin floor. Rest of the balls distributes averagely around the center one. The aim is to suppress the twist effect of the workpiece caused by the non-coaxial of the cutter axis and the support head axis as shown in Fig. 9. All the balls have a diameter of 15mm. Each universal ball is fixed on the head of a piston rod of a small pneumatic cylinder. The small pneumatic cylinder at the back of each ball makes the ball have a small displacement along the axial direction of the cylinder, which makes the support can be applied to the workpiece with curved surface.

The control structure of the whole experimental setup is shown in Fig. 14. The whole control structure is composed by the master control system and the slave control system. The master control system, which is used to control the milling robot, is divided into the motion control of the robot and the spindle control respectively. The cutting path will be generated by the master control system [27, 28]. The following path of the support head is obtained according to the cutting path by considering the workpiece thickness. The motion control and support control is realized by control the joint variable of the support robot, which is solved according to the inverse kinematics.

The real experimental platform is built according to the CAD model and the above described control principle, as shown in Fig. 15.

3.2 Cutting conditions

To verify the effectiveness of the new method, a cutting test is implemented on the developed equipment. For simplicity, a planar workpiece with dimension 1000 mm×1000 mm×15 mm is used during machining is clamped on the worktable. The workpiece material is Aluminum alloy 6061.

A triangular pocket as shown Fig. 16 is machined at the center of the planar workpiece. During machining process, acceleration sensors are attached to the back surface of the workpiece to measure the acceleration signals. Two acceleration sensors are used in total during cutting test. Considering the interference between the moving support head and the acceleration sensors, the acceleration sensors are placed at the area of back surface of the plate that near the cutting zone. Since the workpiece is too large

that can't be fixed on the dynamometer, the machining force signals are not taken in this investigation. After the machining is finished, the machined surfaces are detected.

The cutter used in the cutting process is a right hand cutter with the diameter equals 16 mm and 3 flutes. The helical angle of the cutter is 50°. The material of the cutter is hard steel. Total length of the cutter is 80 mm. The cutter is clamped with the overhang equals to 25 mm. Cutting tests are conducted on the workpiece with and without moving support using the parameters as listed in Table 2 and the cutting path used in the tests is shown in Fig. 16. The cutting parameters listed in the Table 2 are chosen though a trial cutting experiment. The trial cutting experimental results shows that chatter will occur if the cutting parameters are employed.

Table 2 The cutting parameters used in this paper.

Axial depth of cut (mm)	Radial depth of cut (mm)	Spindle speed (rpm)	Feed velocity (mm/min)
0.5	5	5000	2000

3.3 Experimental results

3.3.1 Chatter vibration

Fig. 18 shows the acceleration signals during machining the thin floor of the pocket structure with and without moving support. From the figure it can be seen that the amplitude of the acceleration with moving support is much smaller than that obtained without support. Besides, the signals are much smoother for the case with moving support. The FFT of the signals are shown in Fig. 19. The main frequency part of the acceleration under moving support is the tooth passing frequency which is $f=234$ Hz and its integer multiple, which shows that the cutting process is stable during machining. The FFT of the signal under the case without support is rather different, except the passing frequency part, other parts like $f=341$ Hz and $f=420$ Hz are also existed, which means that the cutting process is unstable and chatter occurs.

3.3.2 Surface quality

The machined surface under different milling conditions is shown in Fig. 20. From the figure it can be seen that the surface quality with the moving support is much better than that without support. The surface roughness $R_a=1.3414$ μm for the case with moving support while it is $R_a=4.0135$ μm for the case without support. This demonstrates the effectiveness of the proposed method to obtain the thin floors with high accuracy during machining the pocket structure.

4. Discussion

Acceleration signals are measured during milling the thin floor with and without moving support. The acceleration signals in time domain are shown in Fig. 18. It can be seen from the figure that the

amplitude of the acceleration when milling without support is much larger than that with support. Fourier transformation results of corresponding acceleration signals in time domain are shown Fig. 19. It also shows the fact that the amplitude of the acceleration that obtained without support is larger than that obtained with support. The introduction of the moving support increases the dynamic stiffness of the whole system which can be denoted as $(\mathbf{K} - \mathbf{M}\omega^2 + \mathbf{C}j\omega)$ where \mathbf{M} , \mathbf{C} and \mathbf{K} , means the system mass, damping and stiffness matrix respectively. The amplitude of the Fourier transformation of the displacement which is $|\mathbf{X}(j\omega)| = |(\mathbf{K} - \mathbf{M}\omega^2 + \mathbf{C}j\omega)^{-1} * |\mathbf{F}(j\omega)|$ will decrease due to the increasing of the dynamic stiffness. And thus the decrease amplitude of the Fourier transformation of the acceleration signals $|\mathbf{A}(j\omega)| = |-\omega^2 * \mathbf{X}(j\omega)|$. Besides, it can be seen from the FFT signals that chatter occurs during milling the thin floor without support since some other frequency components that are not tooth passing frequency exist, while the chatter is successfully suppressed during milling with moving support. This can also be demonstrated by the machined surface topography as shown in Fig. 20, in which irregular marks is shown during milling without support while for the case of using support, only regular cutting marks are observed.

This investigation proposes to use the moving support to strength the local stiffness of the thin floor during its milling process and successfully realize by two robots. The experimental results also show the validation of the proposed method. However, some details about this method should be studied in deeply. In the future investigation, following aspects will be taken into consideration:

- How to control the contact force still remains a major challenge. The contact force between the support element and the thin floor can't be too large or too small. If it is too large, there will be scratch on the back surface of the thin floor. If it too small, the cutter and the floor will still be separated. Recently, the authors tried to use the air jet as the moving support.
- How to choose a proper axial depth of cut is also a challenge. The axial depth of cut can't be too large or too small. If it is two large, the floor will become thinner and thinner. If it is too small, the production will be limited.

5. Conclusions

This paper proposes a novel method to machine the thin floor of a pocket structure. The method is realized by placing a support at the back side of the workpiece. During milling process, the support will move with the cutting tool at the same velocity. Based on this idea, an experimental setup is constructed. It is composed by two five-degree-of-freedom robots where one is equipped with a milling head while the other is equipped with a support. A novel support device is designed to avoid the workpiece twist caused by the non-coaxial of the cutter axis and the support axis. Cutting experiments are implemented on the newly built experimental setup. The experimental results showed that the chatter during milling the thin floors of the pockets can be suppressed by the developed novel system. Besides, surface quality of the floor is much better than that obtained by the traditional machining method. All these demonstrate the validation of the proposed method.

Declarations

Acknowledgements

The experimental platform is constructed with the help of Dr. Chenglin Dong by CAD design, Dr. Qi Liu by programming control. Dr. Hao Guo is also thanked for providing help for conducting the cutting experiments. During preparing this paper, Muhammet Ozsoy, from Department of Mechanical Engineering, The University of Sheffield, Mappin Street Sheffield S1 3JD, UK gives many valuable suggestions to improve the paper quality. The authors thank his contributions.

Funding

This work was financially supported by the National Basic Research numbered 2014CB046603.

Data availability

All data generated or analyzed during this study are included in this published article..

Ethical approval : not applicable.

Consent to participate: not applicable.

Consent to publish: all authors give their consent for the publication of the manuscript.

Competing interests: the authors declare no competing interests.

References

- [1] Wang X, Bi Q, Zhu L, Ding H. Improved forecasting compensatory control to guarantee the remaining wall thickness for pocket milling of a large thin-walled part. *Int J Adv Manuf Technol* 2016; 94(5-8):1677-88.
- [2] Schmitt RH, Peterek M, Morse E, et al. Advances in Large-Scale Metrology – Review and future trends. *CIRP Ann-Manuf* 2016; 65(2):643-65.
- [3] Zhang J, Lin B, Fei J, et al. Modeling and experimental validation for surface error caused by axial cutting force in end-milling process. *Int J Adv Manuf Technol* 2018; 99(1):327-35.
- [4] Gonzalo O, Seara JM, Olabarrieta E, et al. Case Study 1.2: Turning of Low Pressure Turbine Casing. *Intelligent Fixtures for the Manufacturing of Low Rigidity Components*: Springer, 2018;25-38.
- [5] Fu Q, Lorite GS, Rashid MM-U, et al. Suppressing tool chatter with novel multi-layered nanostructures of carbon based composite coatings. *J Mater Process Technol* 2015; 223:292-8.

- [6] Kolluru K, Axinte D. Novel ancillary device for minimising machining vibrations in thin wall assemblies. *Int J Mach Tools Manuf* 2014; 85(7):79-86.
- [7] Kolluru K, Axinte D, Becker A. A solution for minimising vibrations in milling of thin walled casings by applying dampers to workpiece surface. *CIRP Ann-Manuf* 2013; 62(1):415-8.
- [8] https://www.mtorres.es/sites/default/files/documentos/fichas-de-producto/Torresmil%26Torrestool_0.pdf.
- [9] Qin G, Zhang W, Wan M. Analysis and optimal design of fixture clamping sequence. *J Manuf Sci Eng* 2005; 128(2):482-93.
- [10] Chaari R, Abennadher M, Louati J, Haddar M. Mathematical methodology for optimization of the clamping forces accounting for workpiece vibratory behaviour. *Int J Simul Multidiscipl Des Optim* 2014; 5:A13.
- [11] Chen W, Ni L, Xue J. Deformation control through fixture layout design and clamping force optimization. *Int J Adv Manuf Technol* 2007; 38(9):860-7.
- [12] Sundararaman KA, Padmanaban KP, Sabareeswaran M. Optimization of machining fixture layout using integrated response surface methodology and evolutionary techniques. *Proc Inst Mech Eng Part C-j Eng Mech* 2015; 230(13):2245-59.
- [13] Yang B, Wang Z, Yang Y, Kang Y, Li X. Optimum fixture locating layout for sheet metal part by integrating kriging with cuckoo search algorithm. *Int J Adv Manuf Technol* 2016; 91(1-4):327-40.
- [14] Liu SG, Zheng L, Zhang ZH, Li ZZ, Liu DC. Optimization of the number and positions of fixture locators in the peripheral milling of a low-rigidity workpiece. *Int J Adv Manuf Technol* 2007; 33(7-8):668-76.
- [15] Zeng S, Wan X, Li W, Yin Z, Xiong Y. A novel approach to fixture design on suppressing machining vibration of flexible workpiece. *Int J Mach Tools Manuf* 2012; 58:29-43.
- [16] Balachandran B. Nonlinear dynamics of milling processes. *Philos T Roy Soc A* 2001; 359(1781):793-819.
- [17] Long X. Loss of contact and time delay dynamics of milling processes. Doctoral dissertation, University of Maryland, 2006.
- [18] Shamoto E, Mori T, Nishimura K, Hiramatsu T, Kurata Y. Suppression of regenerative chatter vibration in simultaneous double-sided milling of flexible plates by speed difference. *CIRP Ann-Manuf* 2010; 59(1):387-90.

- [19] Mori T, Hiramatsu T, Shamoto E. Simultaneous double-sided milling of flexible plates with high accuracy and high efficiency—Suppression of forced chatter vibration with synchronized single-tooth cutters. *Precis Eng* 2011; 35(3):416-23.
- [20] Fei J, Lin B, Xiao J, et al. Investigation of moving fixture on deformation suppression during milling process of thin-walled structures. *J Manuf Processes* 2018; 32:403-11.
- [21] Fei J, Lin B, Yan S, et al. Chatter mitigation using moving damper. *J Sound Vib* 2017; 410:49-63.
- [22] Ozturk E, Barrios A, Sun C, Rajabi S, Munoa J. Robotic assisted milling for increased productivity. *CIRP Annals* 2018; 67(1):427-30.
- [23] Huang T, Dong C, Liu H, Sun T, Chetwynd DG. A simple and visually orientated approach for type synthesis of overconstrained 1T2R parallel mechanisms. *Robotica* 2018:1-13.
- [24] Huang T, Chenglin D, Liu H, et al. Five-degree-of-freedom hybrid robot with rotational supports, US Patent, US9943967B2, 2018.
- [25] Dong C, Liu H, Yue W, Huang T. Stiffness modeling and analysis of a novel 5-DOF hybrid robot. *Mech Mach Theory* 2018; 125:80-93.
- [26] Xiao J, Xu F, Zhao S, Huang T, B L. An integrated pneumatic rigid mirror milling flexible support device for real-time measurement of thickness, China Patents, 2017.
- [27] Liu Q, Huang T. Inverse kinematics of a 5-axis hybrid robot with non-singular tool path generation. *Robot Cim-int Manuf* 2019; 56:140-8.
- [28] Liu Q, Xiao J, Yang X, Liu H, Huang T, Chetwynd DG. An iterative tuning approach for feedforward control of parallel manipulators by considering joint couplings. *Mech Mach Theory* 2019; 140:159-69.

Figures

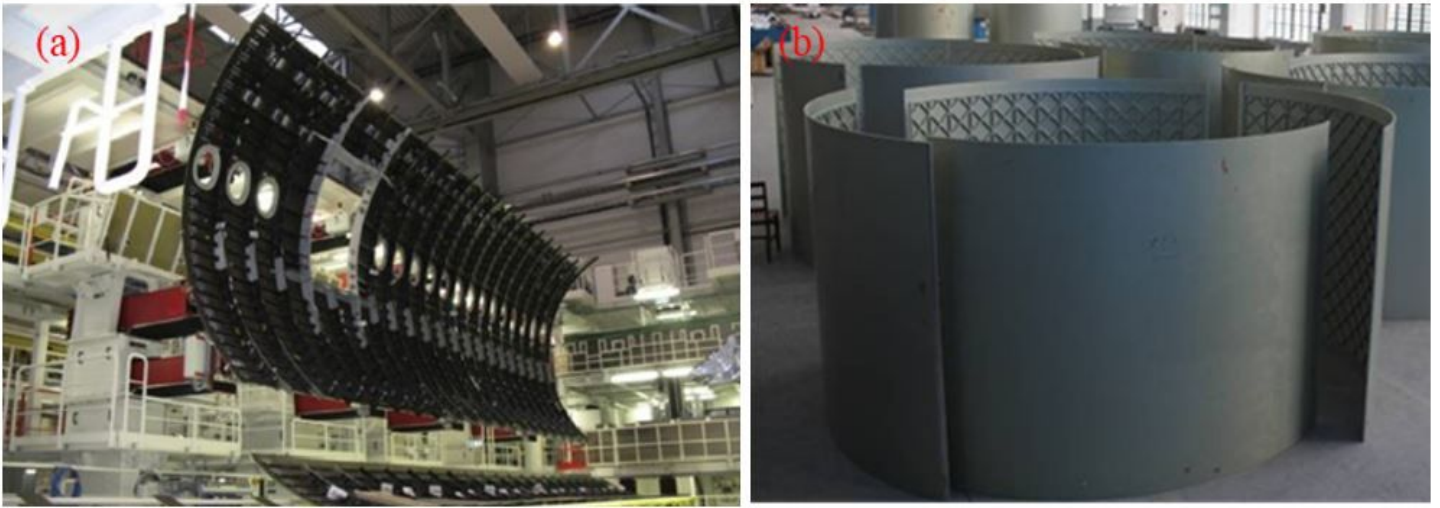


Figure 1

Typical monolithic components with multi-pockets: (a) airplane fuselage [2]; (b) rocket tanks.



Figure 2

The first method to manufacture the large monolithic components with multi-pockets

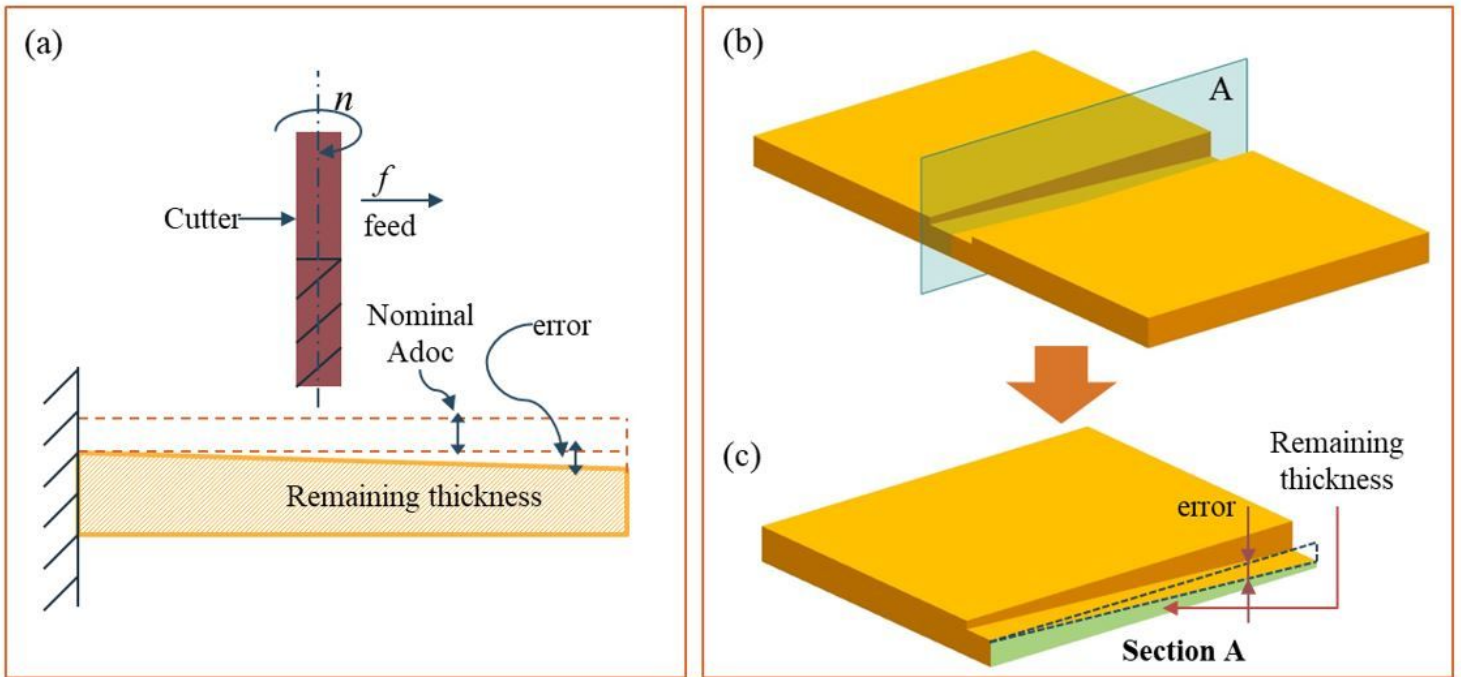


Figure 3

The deformation during thin floor machining and the remaining thickness

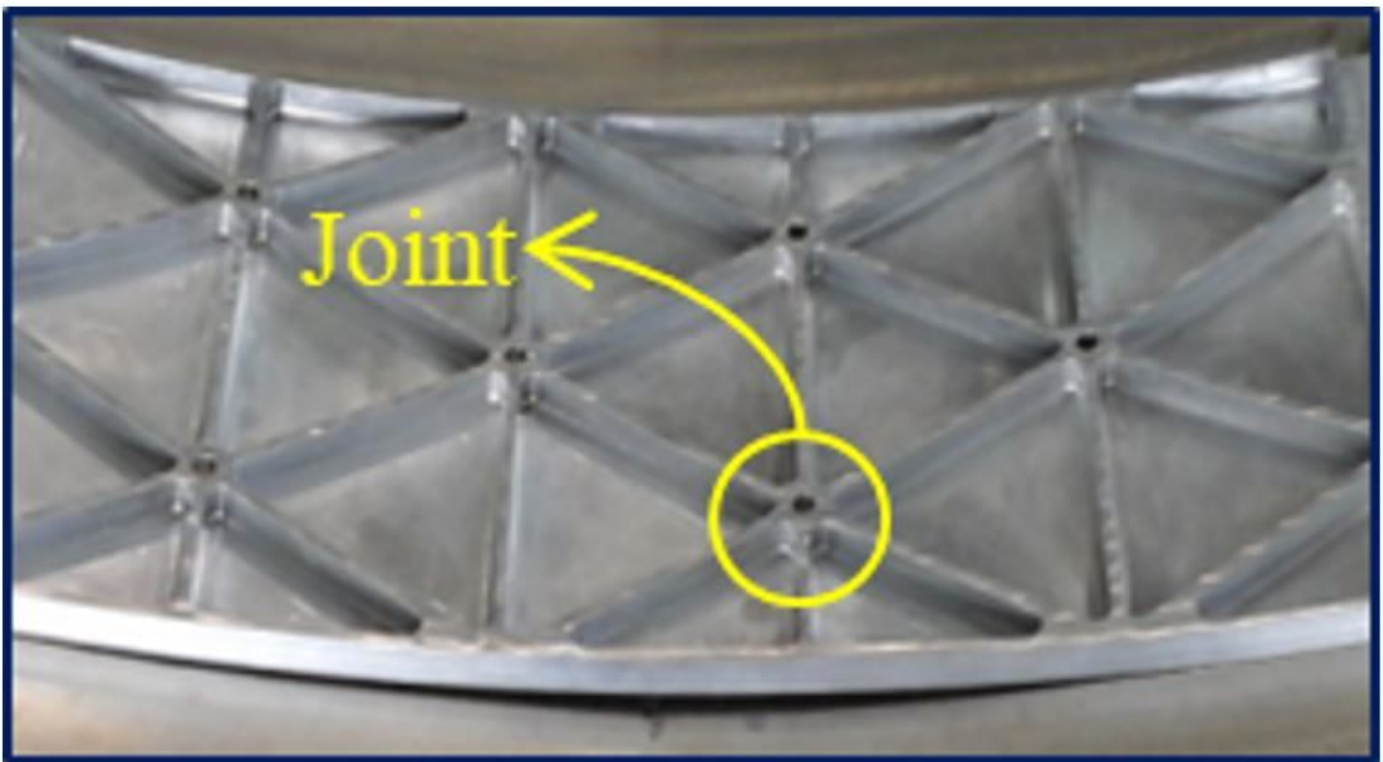


Figure 4

The joint part of the several ribs.

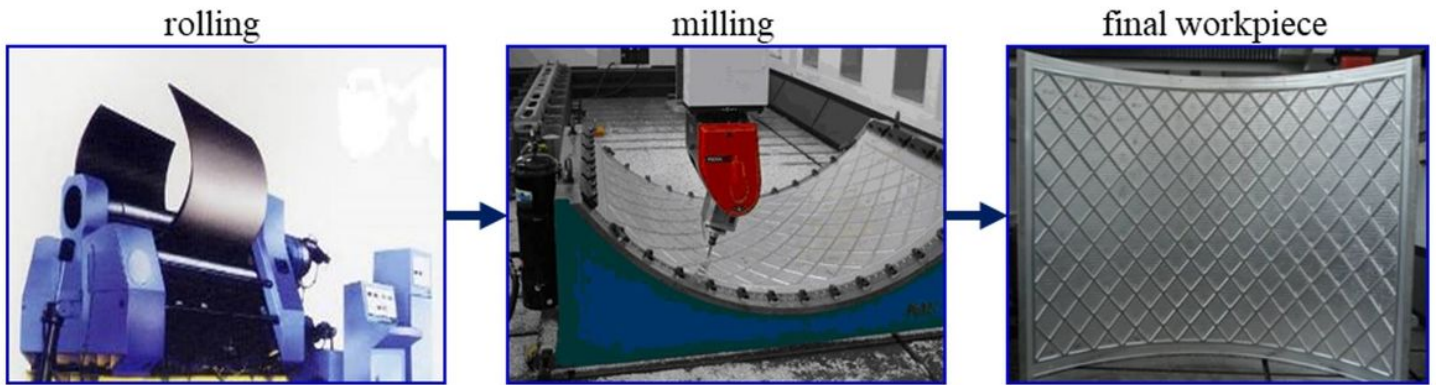


Figure 5

The second method to manufacture the large monolithic components with multi-pockets.

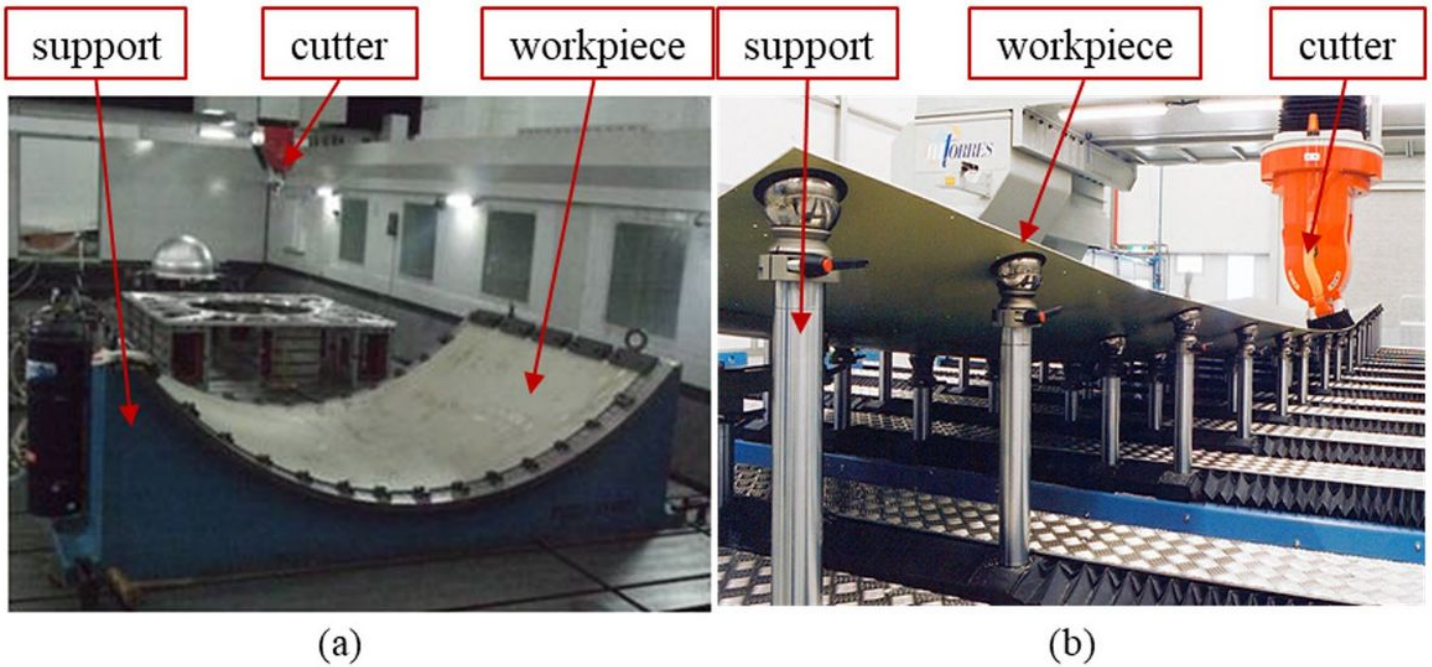


Figure 6

Different methods to strengthen the stiffness of the thin floor: (a) mold design method; (b) matrix support [8].

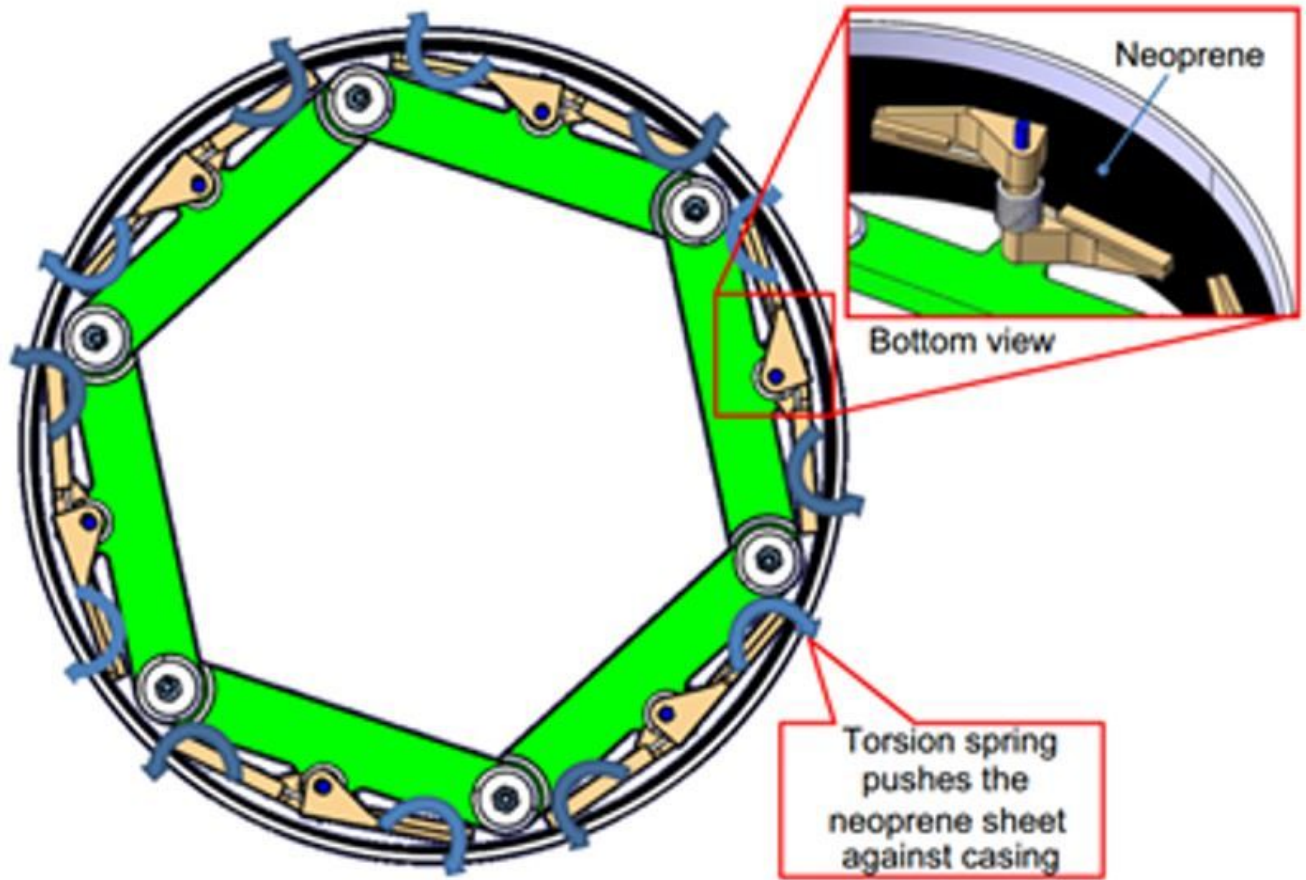


Figure 7

Method proposed by Kolluru and Axinte [6].

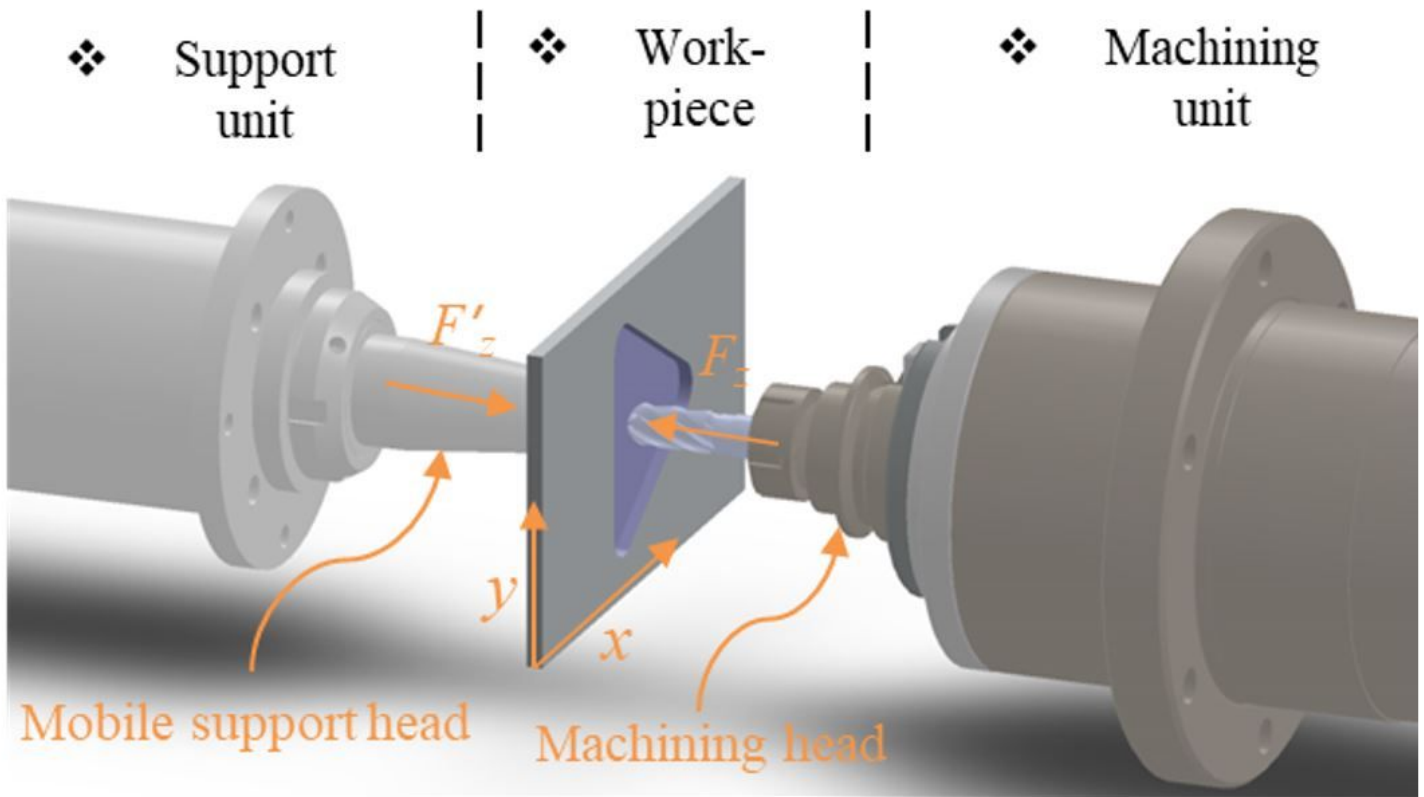


Figure 8

The schematic of the proposed method.

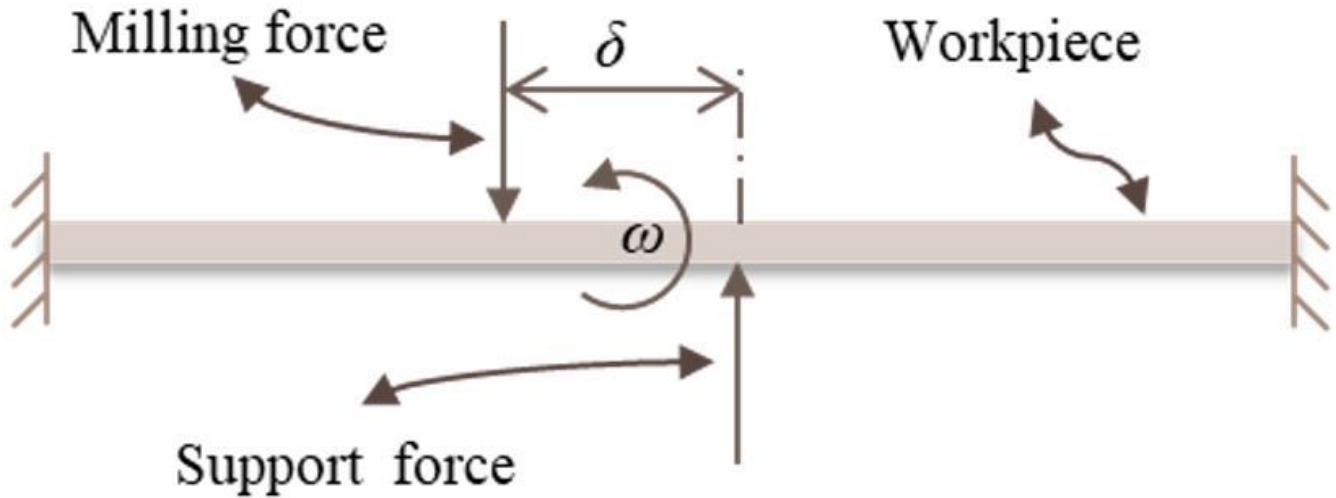


Figure 9

Twist caused by the non-coaxial between the milling force and the support force.

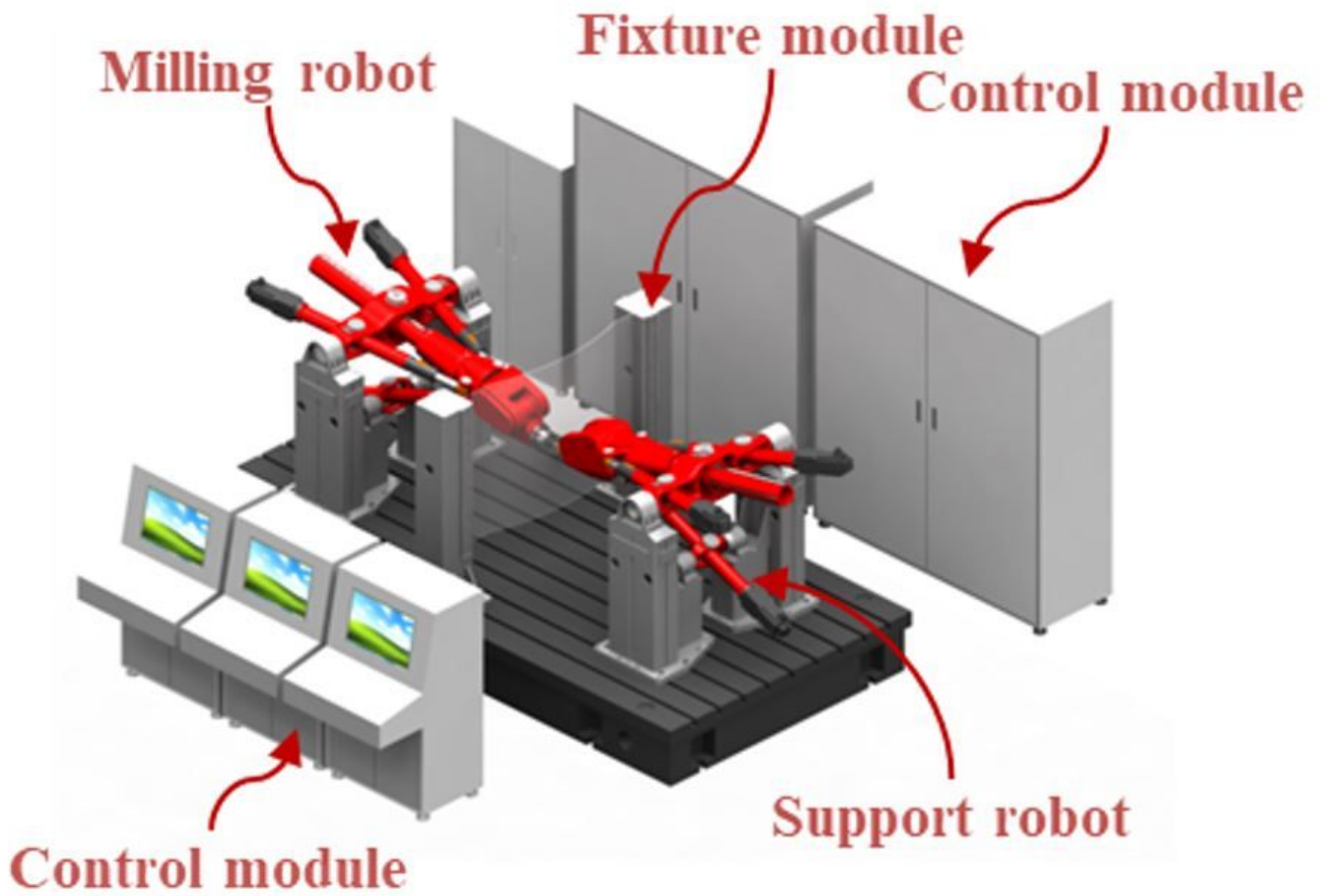


Figure 10

The CAD model of the proposed method.

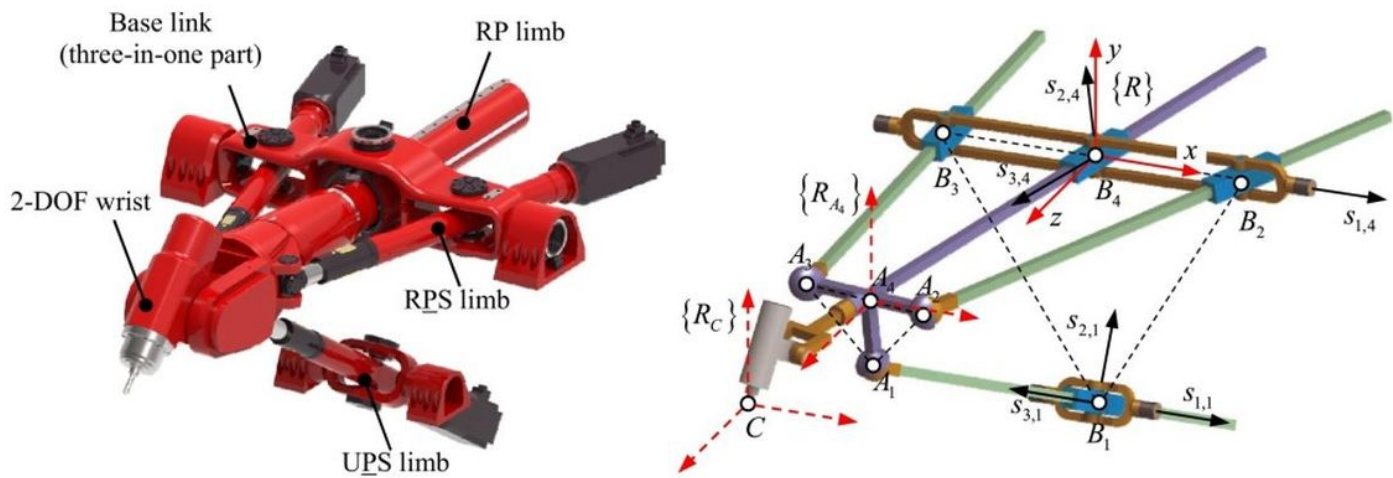


Figure 11

The milling robot and its the mechanism schematic diagram [25].

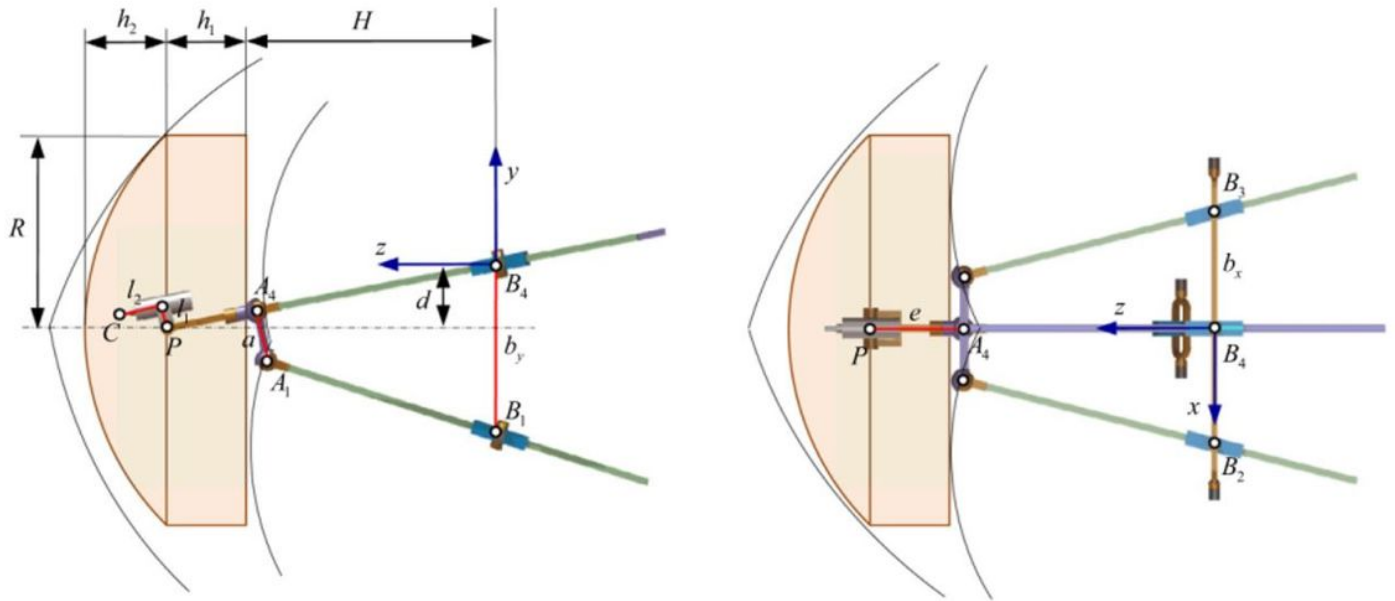


Figure 12

The task workspace of the end effector [25].

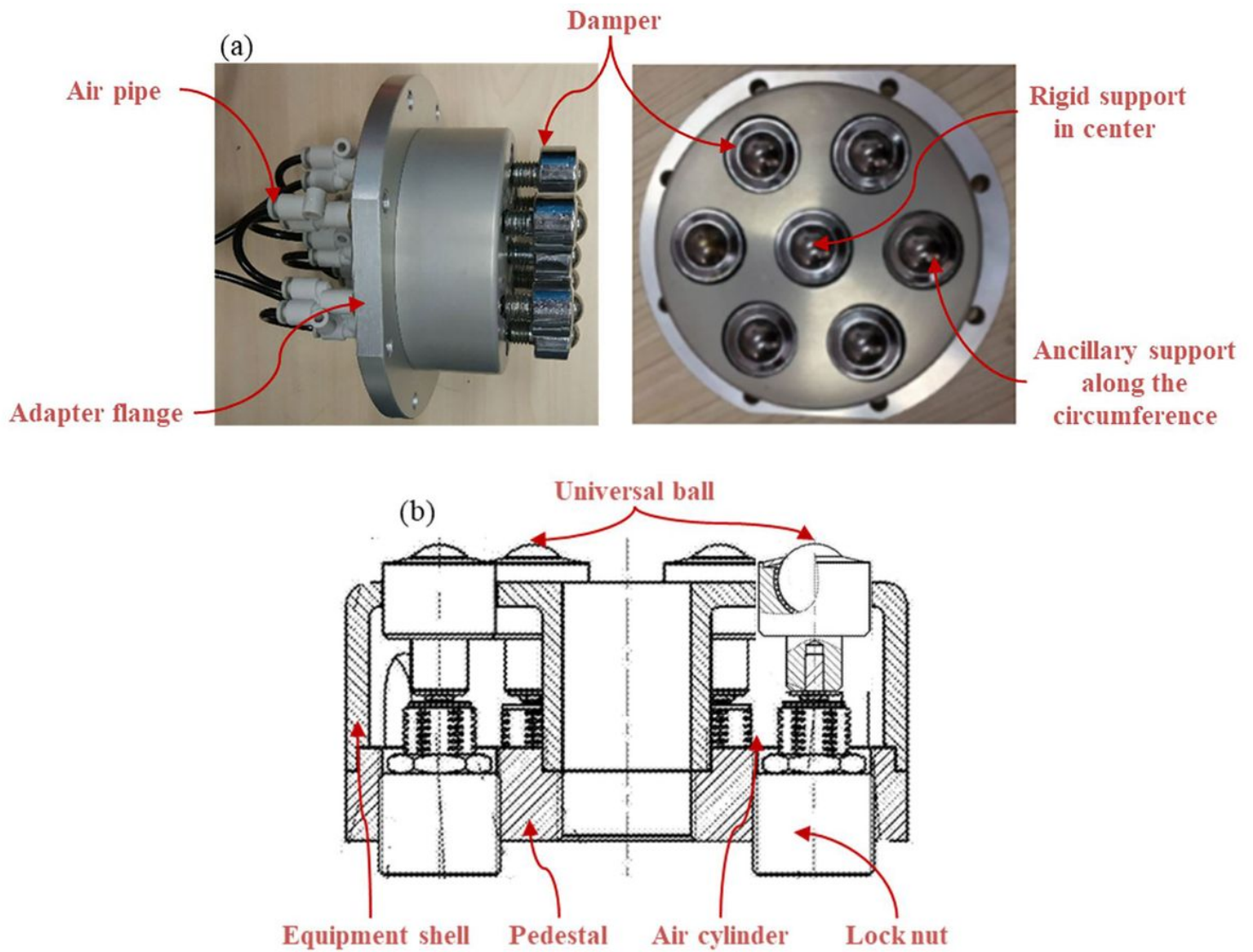


Figure 13

The real support head (a) and the internal structure of the support head (b).

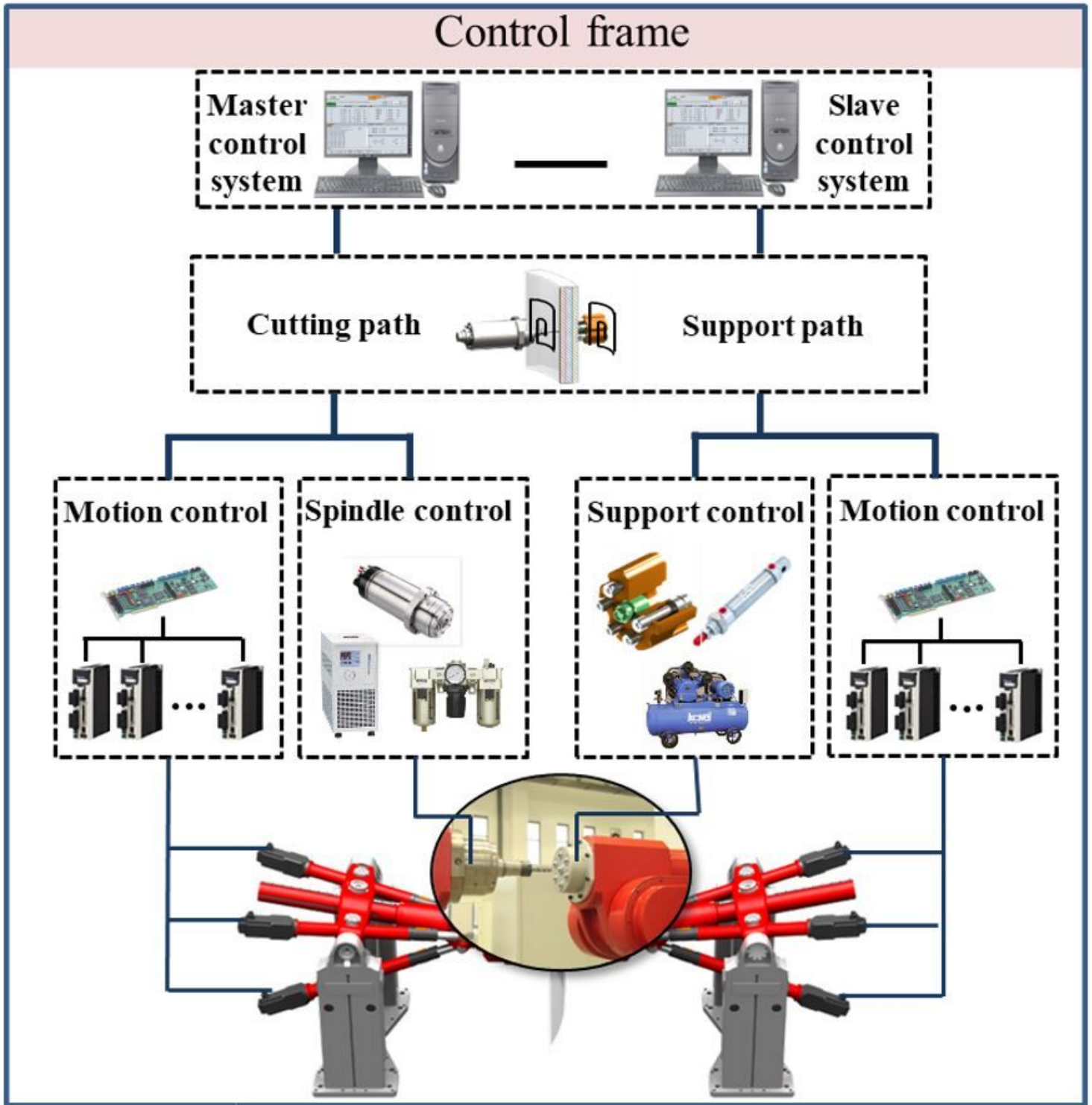


Figure 14

The control structure of the whole system.

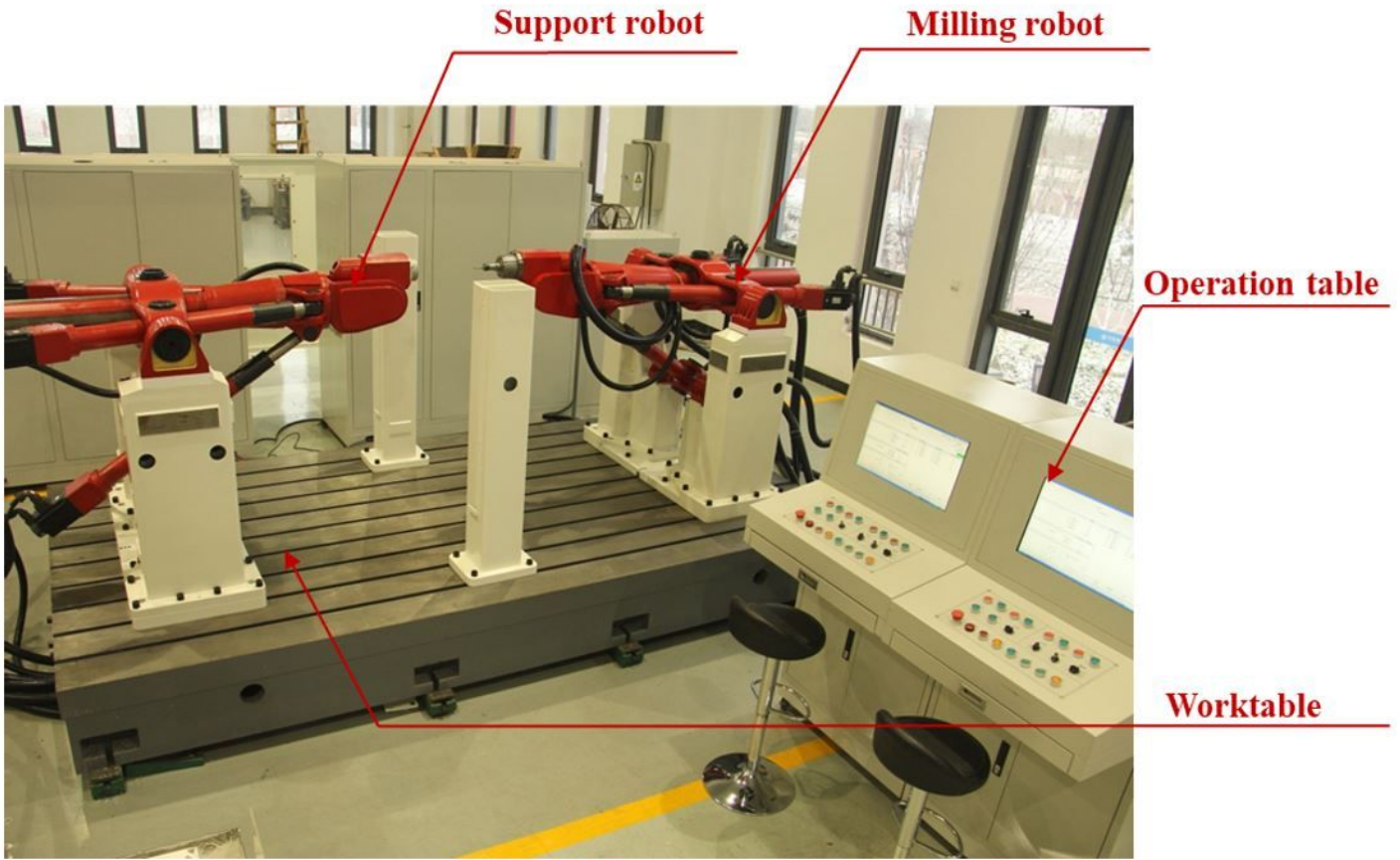


Figure 15

The real experimental platform.

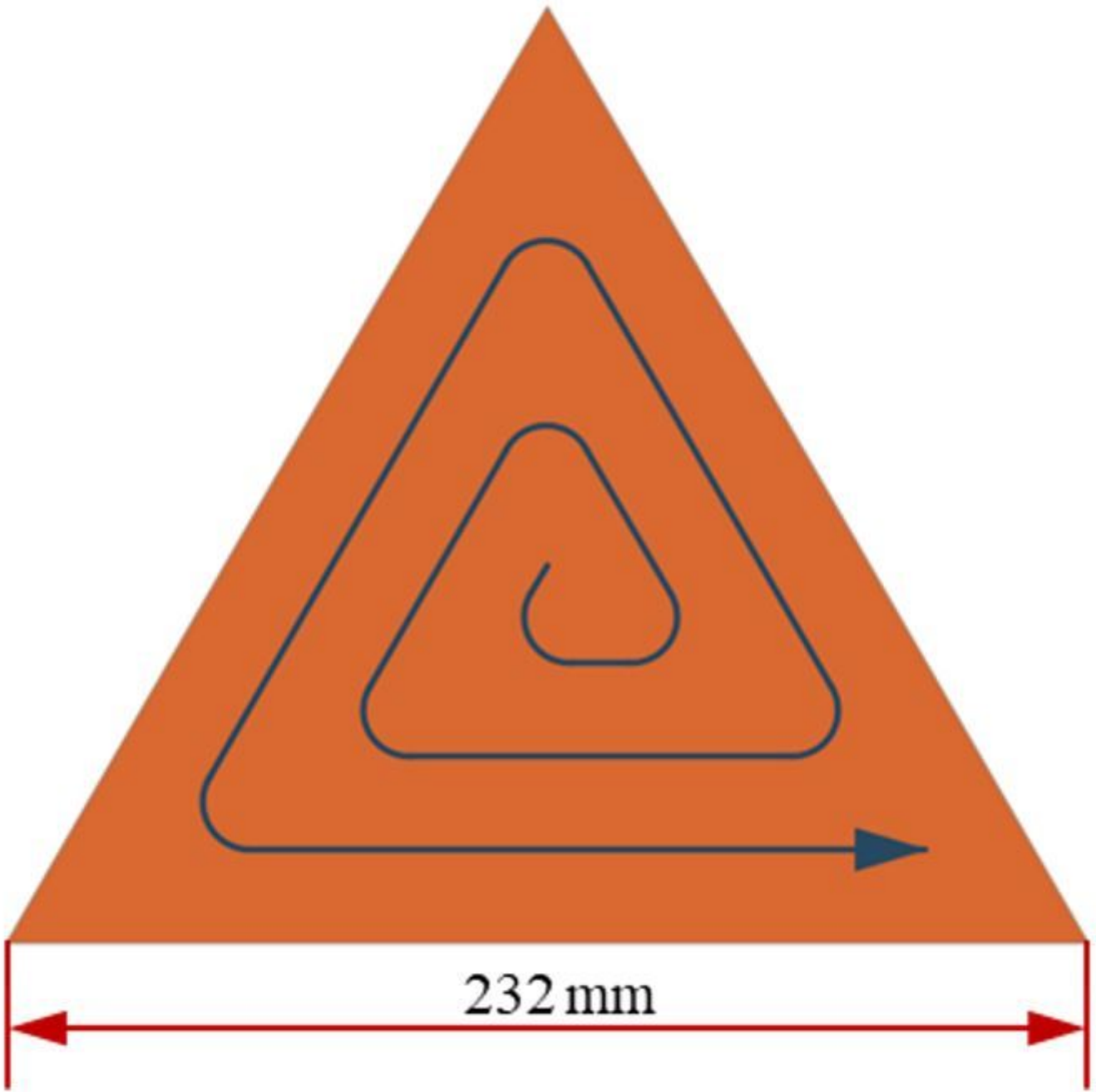


Figure 16

The pocket structure dimensional.



The pocket structure



Acceleration sensors

Figure 17

The real experimental platform.

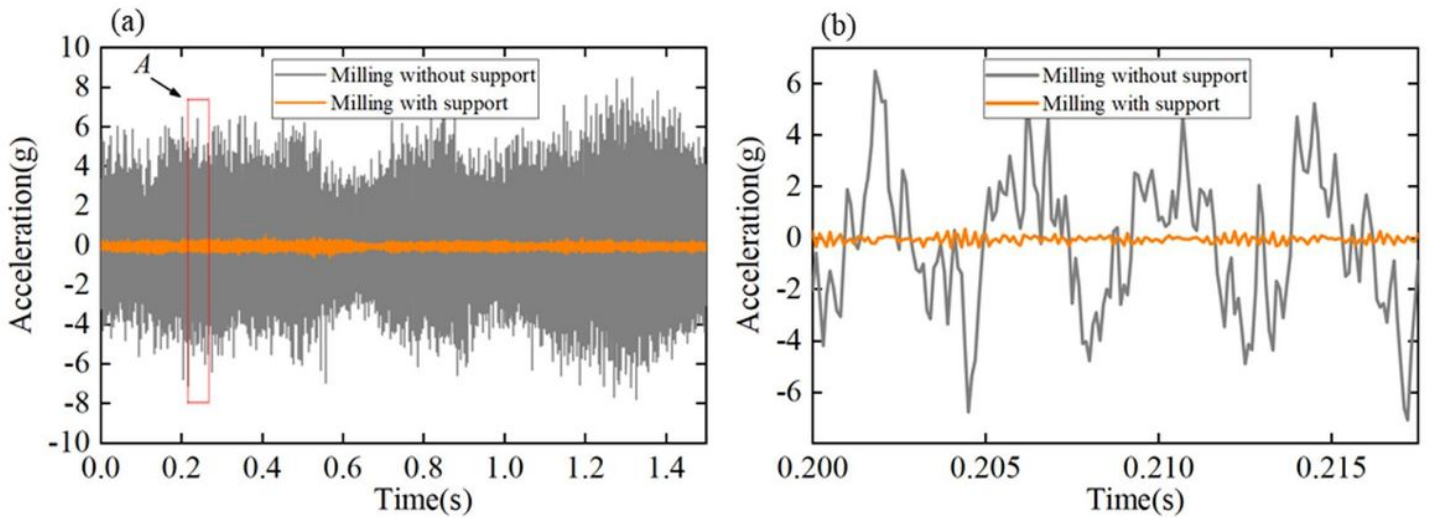


Figure 18

The acceleration comparison: (a) the whole time series; (b) magnification of time period A.

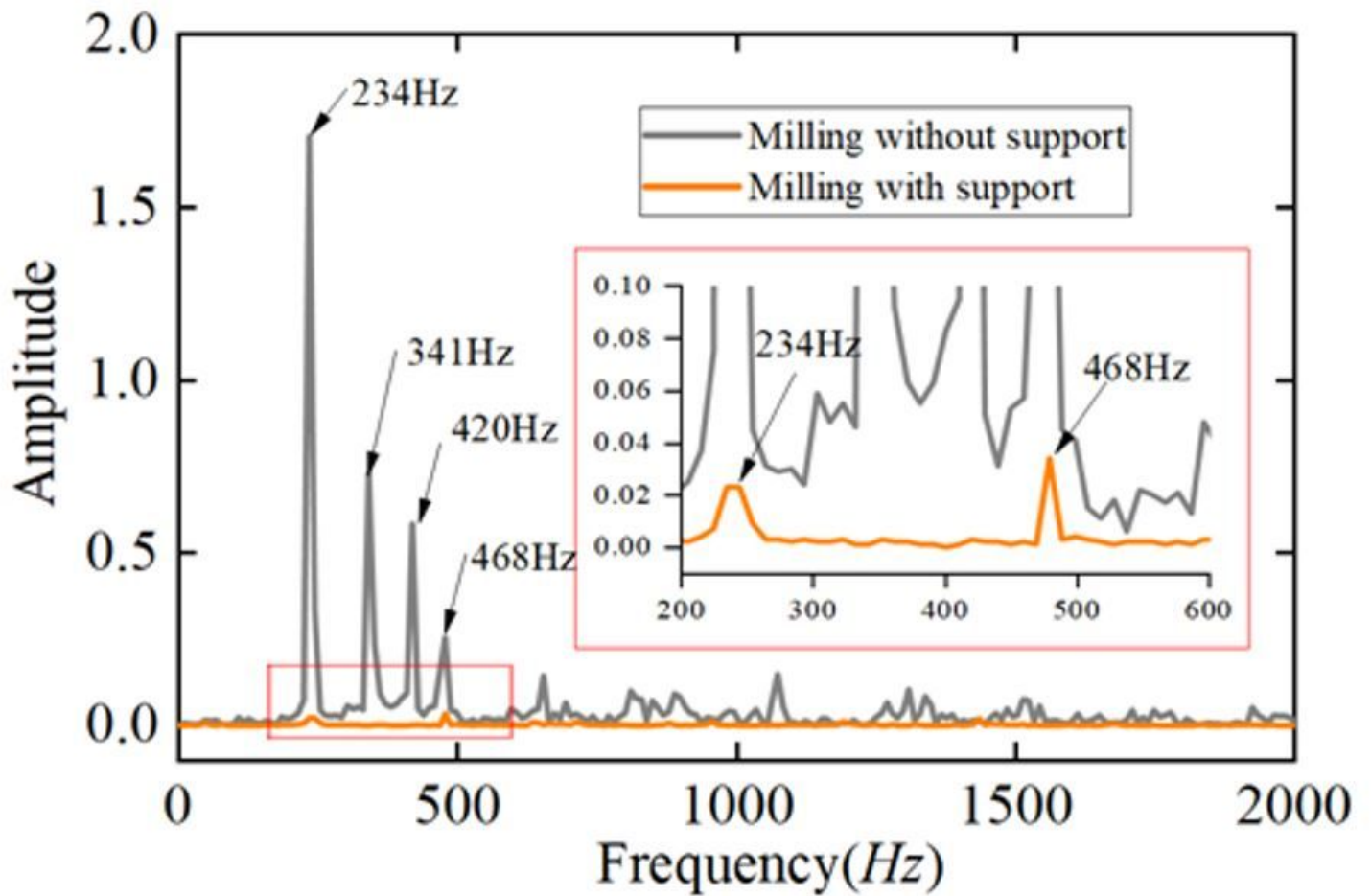


Figure 19

FFT of the acceleration signals.

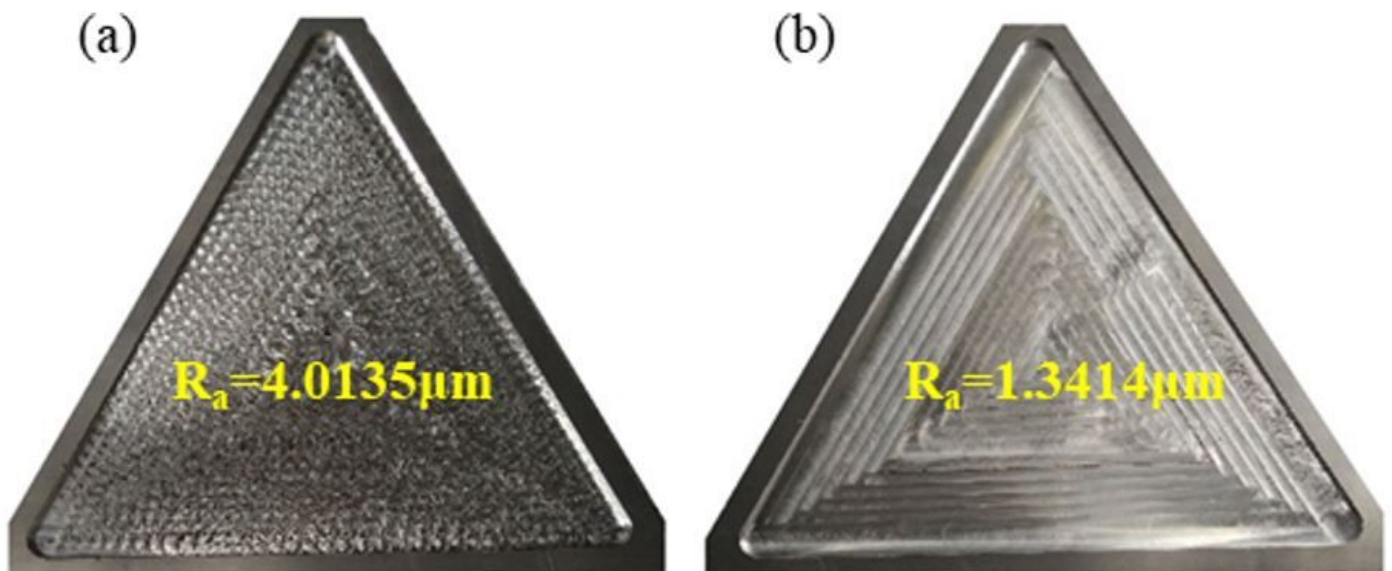


Figure 20

The machined surface: (a) without support; (b) with moving support.